UDC 625.151.2.001.4, 531.01
DOI: 10.15587/1729-4061.2019.154864

STUDYING THE RAILROAD TRACK GEOMETRY DETERIORATION AS A RESULT OF AN UNEVEN SUBSIDENCE OF THE BALLAST LAYER

O. Nabochenko
PhD*
E-mail: olganabochenko@gmail.com
M. Sysyn
PhD, Associate Professor
Department of Planning and Design of Railway Infrastructure
Dresden University of Technology
Hettnerstraße, 3/353, Dresden, Germany, D-01069
E-mail: mykola.sysyn@tu-dresden.de
V. Kovalchuk
PhD*
E-mail: kovalchuk.diit@gmail.com
Yu. Kovalchuk
Assistant**
E-mail: tzov.lviv.bud@gmail.com
A. Pentsak
PhD, Associate Professor**
E-mail: apentsak1963@gmail.com
S. Braichenko
PhD, Senior Lecturer**
E-mail: Lpi2015@ukr.net
*Department of Rolling Stock and Track
Lviv branch of Dnipropetrovsk National University of Railway Transport named after Academician V. Lazaryan
I. Blazhkevych str., 12a, Lviv, Ukraine, 79052
**Department of Construction Industry
Lviv Polytechnic National University
S. Bandery str., 12, Lviv, Ukraine, 79013

Розроблено метод розрахунку розладнання геометрії колії під дією динамічних навантажень при проходженні рухомим складом нерівності колії. Метод враховує взаємопов'язані короткотривалі процеси динамічної взаємодії та довготривалі процеси осідання баластного шару у взаємному впливі один на одного. В основі першої частини методу закладено математичну модель динамічної взаємодії колії у вигляді плоскої тришарової континуальної балкової системи у взаємодії із двохмасовою дискретною системою, що відповідає рухомому складу. Дана модель дозволяє імітувати динамічні навантаження від окремих шпал на баласт при проходженні рухомим складом геометричних нерівностей та нерівностей нерівнопружності колії.

В основі другої частини методу закладено феноменологічну математичну модель накопичення залишкових деформацій, яка ґрунтується на лабораторних дослідженнях осідань окремих шпал у баластному шарі. Особливістю даної моделі є врахування не тільки рівномірного накопичення залишкових осідань із пропущеним тоннажем, а також наявності пластичної складової осідання, яка залежить від максимальних напружень в історії навантажень баласту під кожною шпалою.

Запропоновано новий теоретичний механізм розвитку нерівності колії, який враховує не тільки залишкові осідання баластного шару, а також виникнення люфтів під шпалами, що призводить до локальної зміни пружності колії. Даний механізм дозволяє враховувати неоднозначний вплив осідань із виникненням люфту під шпалою. З однієї сторони, осідання спричинюють збільшення динамічних навантажень на колію і баластний шар, з іншої – виникнення люфту призводить до зменшення жорсткості колії та відповідного зменшення динамічних навантажень.

Практичне застосування розробленого методу показано на прикладі кількісної оцінки довготривалих нерівномірних осідань баластного шару при зміні епюри шпал

Ключові слова: залізнична колія, баластний шар, рухомий склад залізниць, геометрична нерівність колії

1. Introduction

Two fundamentally different types of tracks are used on the world railways: with a ballast layer and with a ballast-free base. The main advantages of the ballast track: relatively low construction costs; easy replacement of track elements; relatively easy correction of the track geometry in routine maintenance; slight adjustments of configuration of the railway track plan are possible; good drainage properties, elasticity and noise absorption.

Cost-efficiency and economy of the ballast track depend on optimal selection of the upper track structure parameters enabling minimal capital and current costs. Assessment of duration of the life cycle of the track and its individual elements is the basis of such selection.

First of all, duration of the life cycle of the ballast track depends on work of one of its main components, namely the ballast layer. The ballast layer is an element of the track which is more likely to be imparted than others and requires running maintenance in the first place. The reason for this is

that the ballast, unlike other elements of the upper structure of the track, is a loose, unbound material that extremely poorly takes dynamic loads. Uneven subsidence of the ballast layer caused by high dynamic loads from the rolling stock leads to impairment of the track geometry which further influences lifecycle of all elements of the track.

The mechanism of development of unevenness of the track geometry as a result of accumulation of residual deformations in the ballast layer is complex and many-sided. Uneven subsidence of the ballast layer depends on many factors of the upper structure of the track, properties of the ballast bed, characteristics of the rolling stock, operating conditions and local atmospheric influences [1].

The process of uneven track subsidence is the result of interconnected processes of sinking of individual sleepers and load redistribution among them caused by formation of gaps under individual sleepers or their groups. As is known [2, 3], sinking of a separate sleeper has a fast in time plastic component and a viscous component depending on the tonnage being passed or the number of axles in the rolling stock. The plastic component of subsidence usually takes place not only at the beginning of the life cycle of the track when stabilization of the ballast layer takes place but also during the life cycle provided that growth of loads on the ballast occurs [4, 5].

Growth of loads on the ballast layer may be caused by a series of factors the main of which is growth of dynamic loading from the rolling stock in the event of the track unevenness. Another factor relates to the occurrence of gaps under the sleepers, that is, a total or partial loss of backing of the sleepers on the ballast. Occurrence of the gap is particularly noticeable in a track with significant local vibrational and dynamic loads in such locations as rail joints, swithes with a rigid bar or short isolated unevenness of the rolling surface [6]. Stress growth in the neighboring sleepers relative to the sleepers with gaps arises as a result of redistribution of loads by the rail-and-sleeper grid. In general, the gap effect is ambiguous. The gap takes loads from separate sleepers on the one hand and causes emergence of an additional elastic unevenness of the track and increases dynamic loads on the other hand.

The mentioned complexity and ambiguousness of the processes taking part in uneven subsidence of the ballast layer and impairment of the track geometry complicate modeling and forecasting of these processes. At present, there is no methodology that would fully take into consideration impairment of the track geometry caused by uneven subsidence of the ballast layer. On the one hand, the existing procedures take into consideration factors of the upper track structure, the rolling stock and operating conditions in the form of design stresses in a procedure [7]. However, introduction of admissible stress values does not enable drawing any conclusions on the loading cycles and inter-repair terms. On the other hand, the methods based on phenomenological models [3, 8, 9-11] do not take into consideration influence of the rolling stock and the track factors although they enable prediction of the track geometry impairment.

2. Literature review and problem statement

Experimental and theoretical studies conducted by a number of authors [1, 2, 8, 12] were devoted to elucidation of impairment of the track and switch geometry.

Uneven subsidence of the ballast layer under sleepers or switch bars has a negative effect on all elements of the railroad track [1, 12]. This is especially true for the elements of sub-rail base, fasteners and sleepers. In the presence of significant uneven subsidence of the ballast layer (Fig. 1), elements of the upper structure of the track are intensively deteriorated (Fig. 2).

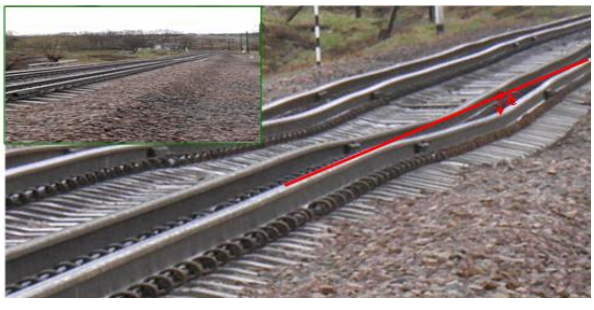

Fig. 1. Impairment of the track geometry caused by the ballast subsidence

Fig. 2. Defects that arise in sleepers in the zone of geometric unevenness of the track

At present, when designing track structures or setting conditions for the rolling stock turnover, efficiency of the ballast layer is estimated by design stresses in the ballast layer and their admissible values which may have different levels depending on the traffic volume and the rolling stock type. This approach of admissible stresses is convenient in solving practical tasks of selecting design and operating conditions but its main drawback consists in the fact that this admissible value does not directly take into consideration operation life of the ballast layer and amounts of running maintenance works.

Another approach is not formulation of certain threshold stresses but establishment of a relationship between these stresses and the loading value. This approach was used in the AASHO-Road-Test study of American Association of State Railways [8] according to which growth of the track loading leads to reduction of the track ballast service life by the fourth-degree dependence:

$$\frac{n_1}{n_2}=\left[\frac{\sigma_2}{\sigma_1}\right]^4, \quad (1)$$

where n_1, n_2 are the numbers of the passed axles at stresses σ_1 and σ_2 at which impairment reaches the same level; σ_1, σ_2 are the specific loads (i. e. design stresses) on the ballast layer.

For example, a 10 % increase in load is equivalent (in geometry impairment) to reduction of the number of passed axles by 32 % [8].

The ORE D141 Committee has developed a method of quantitative calculation assuming that impairment of the track geometry is a power function of loading in accordance with [2]:

$$E = kT^{\alpha}P^{\beta}V^{\gamma}, \quad (2)$$

where E is the increase in the track operation costs caused by impairment after restoration or the last maintenance operation; T is the passed tonnage; P is the total axial load (a sum of static and dynamic loads); V is the speed of movement; k, α, β, γ are constants. Parameters α, β were determined empirically by the ORE D141 and ORE D17 Committees.

From the above procedures, one can see significant distinctions in estimation of the impact of loads and stresses on impairment of the track geometry. This is explained by the fact that these procedures were developed on the basis of generalization of observation of the railway track of a particular design under certain operating conditions. Except operational factors, no factors of design of the upper structure of the track were taken into consideration. At the same time, state of the ballast bed and vibratory effect of the rolling stock exerts a significant influence on impairment of the track geometry [2].

It was established in [2] that impacts result in redistribution of the ballast particles and cyclic loads further increase subsidence of the de-compacted ballast.

Also, changes in geometry of the track and its subsidence depending on the degree of contamination of the ballast after passage of 100,000 axles with a load of 33 t/axis were established in [2]. It was found that with increase in macadam contamination from 0 to 40 %, the track begins to progressively subside and, along with this, vertical unevenness proportionally grows.

Statistical model of forecasting geometric state of switches based on the sequential Monte Carlo method was proposed in [9]. Unlike the conventional phenomenological models, this method enables obtaining of a probabilistic result of geometry impairment based on initial probabilistic values. This, in turn, allows one to forecast the track state for a longer term compared to the conventional regression models.

Study [13] presents simulation of the track geometry impairment caused by differential subsidence of the ballast and the ballast bed based on the iterative approach to calculation of short-term dynamic interaction and long-term processes of accumulation of deformations in the railroad track. The model is represented as a single-layer beam diagram with elastic and viscous elements of the beam supports. As a result, the shape of subsidence unevenness for various numbers of passed axles is obtained.

It was shown in [3] that variable rigidity of the lower track structure plays a decisive role in impairment of the track geometry since, on the one hand, it leads to an increase in dynamic loads from wheels on the track and, on the other hand, it is a direct cause of uneven subsidence of the ballast layer and the ballast bed. It was established that uneven subsidence of the track ballast is caused by heterogeneity of the ballast body. Wadding machines for aligning the vertical profile only temporarily improve it. Moreover, measures are needed that significantly effect rigidity of the subrail base.

Author of [3, 13] has conducted a 100-day observation of development of the track unevenness at various road sections. It was found that impairment of the track geometry depends on the properties of the lower track structure, the ballast layer state, the rolling stock speed and the bending rigidity of rails. It was established that average increase in unevennesses ranged from 0.16 mm to 1.08 mm in 100 days.

Large-scale field tests included studies of the ORE D117 (Office for Research and Experiments of the International Union of Railways) [14] which monitored development of change of geometric position of the track after passage of working loads on railways of Czechoslovakia, France, Poland, Germany and Sweden. It was found that the relative mean square error in subsidence and its variation during tonnage transportation at different railway sections is different. It ranges from 10 % to 40 %.

Laboratory studies [4, 5] have shown that two components can be distinguished in residual ballast subsidence under individual sleepers: viscous and plastic. The plastic component features rapid accumulation of deformations and their fade-out in a relatively short initial time of stabilization. The viscous component has an effect only when the load is long-term, that is, at a simultaneous influence of the factor of the number of passed axles takes place.

Uneven subsidence of the ballast layer has two consequences: appearance of geometric unevenness of the track and gaps under sleepers [15]. The gap impact is double. It greatly increases intensity of subsidence on the one hand and leads to emergence of an additional non-uniformity of the track rigidity on the other hand. As a result, force variation increases which, together with geometric unevenness, creates unevenness in the railway track and switches. Thus, uneven subsidence has a reverse effect because of gap formation. On the one hand, it accelerates intensity of subsidence and, on the other hand, it starts reduction of the sleeper pressure on the ballast up to a complete unloading at a value sufficient for these effects.

Unevenness of the rail rolling surface has an additional reverse effect caused by additional dynamic loading and additional dynamic pressure of sleepers on the ballast. In addition to the depth of subsidence, dynamic load is influenced by the length of unevenness which is considered unchanged and depending only on external factors of the track structure and the rolling stock factors. To simplify calculations, unevenness slope is taken as the unevenness parameter influencing the dynamic load.

It can be concluded from analysis of the published data that the problem of forecasting impairment of the track geometry resulted from uneven subsidence of the ballast layer was not fully solved in practical and theoretical terms. The least studied are the long-term processes of uneven residual deformations in the ballast layer which, in turn, cause impairment of the track geometry during passage of tens of million tons of cargo. The effect of gap in the sleeper work is even less studied. It is connected with the process of redistribution of loads from sleepers to the ballast and the change of dynamic loading from the rolling stock caused by the change of the track elasticity.

Solution of the theoretical side of the problem is closely connected with the practical task of establishing quantitative interrelations between parameters of the track structure and their effect on the long-term impairment processes. The pressing practical task consists in estimation of the effect of the sleeper diagram on lifetime of the ballast layer and the cost of maintaining the railroad track.

3. The aim and objectives of the study

The study objective was to ascertain influence of the ballast layer on the railway track geometry impairment.

To achieve this objective, the following tasks had to be solved:

– develop a mathematical model of interaction of the track with the railway rolling stock taking into consideration viscous and plastic properties of the ballast layer as well as the influence of vibration loads on them;

– develop a model of residual subsidence of the ballast layer under the influence of multiple cyclic and short-term dynamic loads;

– perform simulation of the ballast state effect on impairment of the railroad track geometry for various sleeper diagrams.

4. Procedure for forecasting residual subsidence of the ballast layer

Residual track deformation or residual vertical unevenness depends on the track loading from the rolling stock, its nature and magnitude. On the other hand, nature and magnitude of the load that arises in a single passage of a vertical unevenness depends on the amount of residual deformation of the ballast layer which causes formation of a gap and a change of the track elasticity. Thus, there is an inverse relationship between these factors which is presented in Fig. 3.

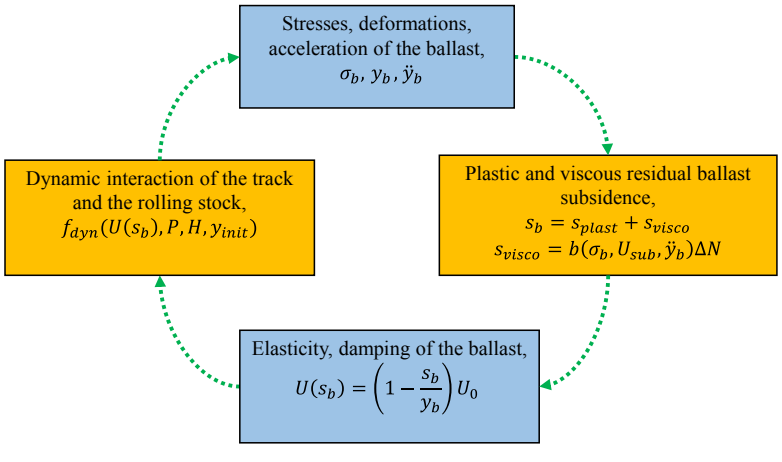

Fig. 3. Diagram of interrelation of short- and long-term processes in the ballast layer

Formally, this relationship can be represented as follows. The initial unevenness y_{init} of a certain small value causes dynamic interaction of the track and the rolling stock which together with static load P makes the force of action on the track:

$$\{\sigma_b, \ddot{y}_b\} = f_{dyn}(U(s_b), P, H, y_{init}), \quad (3)$$

where P is the rolling stock characteristics and speed; H is the track characteristics; σ_b is the dynamic stresses in the ballast; $\ddot{y}_b$ is acceleration of the ballast layer; $U(S_b)$ is the properties of elasticity and damping of the ballast layer; s_b is residual deformations in the ballast layer.

Depending on the stresses, accelerations and the number of loading cycles, residual deformations in the ballast layer are determined on the basis of experimental measurements [16].

Behavior of subsidence is described by summation of the plastic component s_{plast} (independent of the time of plastic subsidence, initial subsidence) and the viscous component s_{visco} (independent of the time of viscous subsidence, secondary subsidence):

$$s_b = s_{plast} + s_{visco}. \quad (4)$$

The plastic component of subsidence, s_{plast}, occurs abruptly and mainly in the initial period of the track stabilization. The component of plastic subsidence, $s_{F\max}$, occurs when the stress in the ballast layer under the sleeper, σ_i, is greater than that which arose up to that time in the history of loading, MAX (σ_i). The magnitude of MAX (σ_i) was determined by the results of laboratory tests given in [16], by loading of a separate sleeper in a sleeper box by a cyclic non-vibration load. The ballast was considered maximally compacted on a rigid ballast bed.

Amplitude of the cyclic loading increased in each subsequent test resulting in an increase in the level of initial subsidence. Complete unloading of sleepers did not occur. The relationship between initial subsidence and maximum load is represented by the approximation dependence as a second-order polynomial:

$$s_{plast} = s_{F\max} = 42{,}953 \cdot \max(\sigma_i)^2 + 5{,}6844 \cdot \max(\sigma_i). \quad (5)$$

The maximum value of the plastic component, $s_{F\max}$, is achieved during loading of 1 million tons. Asymptotic dependence of the ballast subsidence on the number of loads was used for this description [15, 16]:

$$s(N) = s_{F\max} \frac{N}{a + bN}, \quad (6)$$

where N is the number of repetitive loads; a=10,000, b=1 are the coefficients that depend on the stressed state and physical properties of macadam.

Viscous behavior of subsidence depends on the number of load changes. At present, there are many simpler and more complex phenomenological formulas of subsidence [3, 4, 15] which give different results and are difficult to be compared. The result of this study is not the absolute value of subsidence but its variation, therefore, a linear dependence on the number of loadings was approximately taken for a simplified description of the viscous component:

$$s_{visco} = b(\sigma_b, U_{sub}, \ddot{y}_b)\Delta N, \quad (7)$$

where ΔN is the increase in the number of load cycles; $b(\sigma_b, U_{sub}, \ddot{y}_b)$ is intensity of accumulation of residual deformations which depends on the stress in the ballast layer, σ_i, under the sleepers, elasticity of the ballast bed, U_{sub}, and accelerations in the ballast layer, $\ddot{y}_b$.

Intensity $b(\sigma_b, U_{sub}, \ddot{y}_b)$ is defined as a product of corresponding components:

$$b(\sigma_b, U_{sub}, \ddot{y}_b) = b(\sigma_b) b(U_{sub}) b(\ddot{y}_b). \quad (8)$$

The component from the stresses in the ballast is determined by empirical formula of polynomial of the third degree obtained in processing the results of experimental tests of VNDIZT [16] for pure macadam with fraction size of 25–60 mm:

$$b(\sigma_i)=1{,}981\sigma_i^3+0{,}199\sigma_i^2+0{,}029\sigma_i \text{ (mm/10,000 axles)}. \quad (9)$$

The component from elasticity of the ballast bed is determined on the basis of study [17]:

$$b(U_{sub})=k_U(U_s)=\frac{6000}{14U_s^{1,29}-26}+0{,}74. \quad (10)$$

An increase in intensity of the ballast layer deformation resulting from the action of accelerations was derived from experimental VNDIZT studies [16] and was described by a simple dependence:

$$b(\ddot{y}_b)=1+0{,}5\left(\frac{\ddot{y}_b}{9{,}81}\right)^{1,4}. \quad (11)$$

Influence of the gap on intensity of the ballast layer deformation was taken into consideration in the model through the change of elasticity and damping of the model elements corresponding to the ballast layer. At present, various approaches to the description of the gap work in the models are known. They are presented in [15]. In this study, the following dependence was taken with account of the multi-sided nature of the process of interaction of sleepers with the ballast in the gap zone:

$$U(s_b)=\left(1-\frac{s_b}{y_b}\right)U_0, \quad (12)$$

where U_0 is initial of elastic and damping properties of the ballast layer; y_b is the elastic deformations in the ballast layer.

This correlation reduces initial elasticity of the ballast layer in the event of gap formation, up to zero, if subsidence is greater than elastic deflection.

Dependence (10) is a formal record of interconnection of the stress-strain state of the track and physical and geometric characteristics of the track and the rolling stock at a certain time. This dependence corresponds to the time of interaction when a car is passing the vertical unevenness of the track. That is, it reflects the short-term interaction of the track with the rolling stock. Dependences (1) to (8) reflect rheological model of accumulation of residual subsidences in the ballast layer over a long period of time.

4. Development of a mathematical model of interaction of the railway track with moving over-spring and under-spring masses

Generalized mechanical system was taken as a car model for modeling dynamic interaction of the track with the rolling stock (Fig. 4). This system consists of two inertial bodies: springed and non-springed masses and reflects passage of one carriage axis. A model consisting from continual inertial Euler beams with their mass concentrated in the beam axles was selected as the track model.

Beams are arranged one upon another and separated by elastic continual layers that correspond to the Winkler's base and have viscous-dissipative properties. The bottom beam is placed on a stationary base [17–20]. Each of the beams corresponds to structural elements: a rail, a sleeper with fastening, a ballast layer with a ballast bed. Action of individual sleepers is described through introduction of spaces with a low value of rigidity and damping in the top fastening layer [21–23].

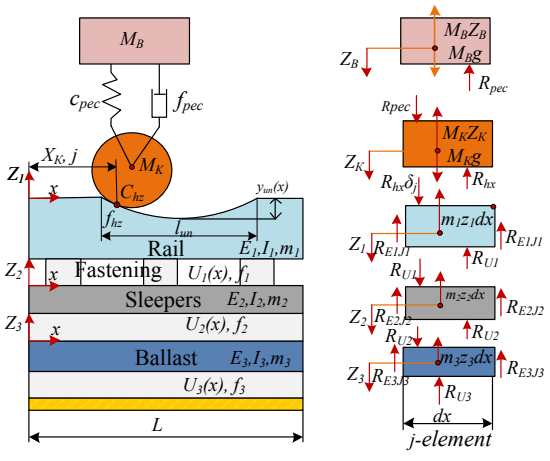

Fig. 4. Calculation diagram of interaction of the track with the rolling stock

The union of n_x elements of a beam into a common beam of length L results in a system of differential equations of n_x power which is written in the matrix form as follows:

$$[\mathrm{M}]\cdot\ddot{Z}+[\mathrm{C}]\cdot\dot{Z}+[\mathrm{K}]\cdot\mathrm{Z}=\mathrm{P}, \quad (13)$$

where P is the matrix of loadings; [M] is the matrix of element masses; [C] is the matrix of damping in connecting layers; [K] is the matrix of rigidities taking into consideration the bending rigidity of the beam and the rigidity from resting; $\ddot{Z}$, $\dot{Z}$, Z are vectors of accelerations, velocities and displacements of the beams elements, respectively.

The matrix of masses [M] has a diagonal form with a nonzero main diagonal. It consists of three square blocks with dimensions $N\times N$ (N is the number of elements into which each beam is sectioned) i. e. $[M_1]$, $[M_2]$ and $[M_3]$ as well two blocks with dimensions 1×1 M_B and M_K that reflect discrete masses of the carriage:

$$[\mathrm{M}]=\begin{bmatrix} M_B & 0 & 0 & 0 & 0\\ 0 & M_K & 0 & 0 & 0\\ 0 & 0 & [M_1] & 0 & 0\\ 0 & 0 & 0 & [M_2] & 0\\ 0 & 0 & 0 & 0 & [M_3] \end{bmatrix}. \quad (14)$$

The matrix of damping [C] has the same form and size as the matrix of masses, however, additional diagonal elements are added to it:

$$[\mathrm{C}]=\begin{bmatrix} [f_{pec}] & -[f_{pec}] & 0 & 0 & 0\\ -[f_{pec}] & [f_{hz}]+[f_{pec}] & -[f_{hz}]\cdot\delta_{1j} & 0 & 0\\ 0 & -[f_{hz}]\cdot\delta_{1j} & [f_1]+[f_{hz}]\cdot\delta_{1j} & -[f_1] & 0\\ 0 & 0 & -[f_1] & [f_2]-[f_1] & -[f_2]\\ 0 & 0 & 0 & -[f_2] & [f_3]+[f_2] \end{bmatrix}. \quad (15)$$

Besides the additional diagonal elements in adjacent non-diagonal blocks, the matrix of rigidity includes additional diagonal elements near the main diagonal because the bending rigidity is introduced to it. The matrix of rigidity has the form:

$$[\mathrm{K}]=\begin{bmatrix} [C_{pec}] & -[C_{pec}] & 0 & 0 & 0 \\ -[C_{pec}] & [C_{hz}]+[C_{pec}] & -[C_{hz}]\cdot\delta_{1j} & 0 & 0 \\ 0 & -[C_{hz}]\cdot\delta_{1j} & [E_1I_1D^4]+[U_{1j}]+[C_{hz}]\cdot\delta_{1j} & -[U_{1j}] & 0 \\ 0 & 0 & -[U_{1j}] & [E_2I_2D^4]+[U_{2j}]+[U_{1j}] & -[U_{2j}] \\ 0 & 0 & 0 & -[U_{2j}] & [E_3I_3D^4]+[U_{3j}]+[U_{2j}] \end{bmatrix}. \quad (16)$$

In matrices (13) and (14) there are elements having a multiplier δ_{1j}. This means that non-zero element of the main diagonal is one that corresponds to the point of contact of the wheel and the rail. The operator D^4 means decomposition of the bending rigidity into a difference scheme.

In addition to the gravitational loading, the function of forces from vertical unevenness is also described in the vector column of external loading, *P*, by the formula:

$$P=\begin{bmatrix} M_Bg \\ -C_{hz}\cdot[y_{un}]\cdot\delta_{1j}-f_{hz}\cdot[\dot{y}_{un}]\cdot\delta_{1j}+M_Kg \\ C_{hz}\cdot[y_{un}]\cdot\delta_{1j}+f_{hz}\cdot[\dot{y}_{un}]\cdot\delta_{1j} \\ 0 \\ 0 \end{bmatrix}. \quad (17)$$

To solve the problem, it is necessary to find the vector of displacements of the system elements:

$$Z=\begin{bmatrix} Z_B \\ Z_K \\ Z_1 \\ Z_2 \\ Z_3 \end{bmatrix}, \quad (18)$$

where Z_B is the vector of displacements of the over-spring mass of the car; Z_K is the vector of displacements of the under-spring mass of the car; Z_1 is the vector of displacements of the top beam elements; Z_2 is the vector of displacements of the middle beam elements; Z_3 is the vector of displacements of the bottom beam elements.

In order to solve the problem, it is necessary to introduce initial and boundary conditions that have the following physical content: the beams are restrained at the edges at any given time moment and velocities of all material points are zero at the initial time moment.

Initial conditions:

$$\begin{cases} z_e(0,t)=0, \\ z_к(0,t)=0, \\ z_1(x,0)=0, \\ z_2(x,0)=0, \\ z_3(x,0)=0, \end{cases} \quad \begin{cases} \dot{z}_e(0,t)=0, \\ \dot{z}_к(0,t)=0, \\ \dot{z}_1(x,0)=0, \\ \dot{z}_2(x,0)=0, \\ \dot{z}_3(x,0)=0. \end{cases} \quad (19)$$

Boundary conditions at the beginning and at the end of the area:

$$\begin{cases} \dfrac{\partial z_1(0,t)}{\partial x}=0, \\ \dfrac{\partial z_2(0,t)}{\partial x}=0, \\ \dfrac{\partial z_3(0,t)}{\partial x}=0, \end{cases} \quad \begin{cases} z_1(0,t)=0, \\ z_2(0,t)=0, \\ z_3(0,t)=0, \end{cases}$$

$$\begin{cases} \dfrac{\partial z_1(L,t)}{\partial x}=0, \\ \dfrac{\partial z_2(L,t)}{\partial x}=0, \\ \dfrac{\partial z_3(L,t)}{\partial x}=0, \end{cases} \quad \begin{cases} z_1(L,t)=0, \\ z_2(L,t)=0, \\ z_3(L,t)=0. \end{cases} \quad (20)$$

Choice of boundary conditions in the form of a system (20) is the most simple, however, it leads to some inconveniences when solving the problem numerically. These inconveniences are related to the so-called initial area of stabilization of oscillatory motion of the model which arises when initial displacements are taken to be zero which does not correspond to reality. In some problems, the initial stabilization area is rejected in a further calculation when displacements caused by initial conditions become insignificant. In the given case, the time spent on stabilization can take up a significant part of simulation time. Therefore, in order to avoid this, masses and damping of all elements in the equation (17) are set close to zero at the first step of the calculation cycle. Thus, the problem of determining static deflections is solved in the first step of the cycle. In this case, there is no accumulation of kinetic energy as in inertial elements and oscillations quickly take the state of equilibrium.

Since restraining of beams at both ends was taken in the role of boundary conditions, application of an external load near the edges also causes a calculation error. In order to avoid this calculation error related to the taken boundary conditions, the point located at a distance of more than 4 m from the beginning of the beam is taken as the starting point of the system reflecting the carriage. At such a distance from the beginning of the beam, impact of restraint on deflection is less than 3 %. The point of completion of movement is also taken at a distance of 4 m from the end of the beam.

Practical implementation of calculation was performed using the Matlab program package [22]. For an example of calculation, let us present the results of simulation of the car movement in a 25 m long track section. When performing calculations, the following initial data were set: M_B= =11,600 kg; M_K=990 kg; m_1=65 kg/m; m_2=250 kg/m; m_3=700 kg/m; E_1=2.1·10^{11} N/m^2; I=3,548·10^{-8} m^4; C_{pec}= =80·10^9 N/m. The system speed was 160 km/h. On the track there was an isolated geometric unevenness in the length of 1.0 m and a depth of 0.5 mm. The sleeper diagram was 1,840 pcs/km. Time sampling was connected with a step taken equal to 0.05 m. Thus, sinusoidal unevenness is described by 13 points which is sufficient for a smooth reflection of unevenness. Forces vary continuously at the point of contact of the wheel and the track. They increase on the unevenness depending on the unevenness parameters.

The diagram of change of the coefficient of soil reaction of the track elements is shown in Fig. 5. The top layer is stepped and reflects the sleeper diagram, the coefficients of soil reaction of the middle and lower layers are constant. All

these values are given as the intensity of loading or the force of action on 1 m along the track axis. It was established that forces arise only in fastenings and there are no forces in the inter-sleeper space. Forces change continuously in the sleeper-ballast layer and the ballast bed while in the ballast there is a smooth increase in pressure under sleepers and decrease in the inter-sleeper space.

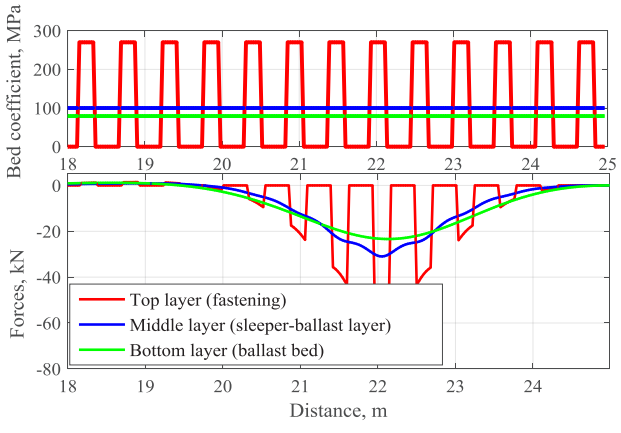

Fig. 5. The diagram of change of bed and force coefficients for fastening, ballast and ballast bed layers

Besides parameters of the stress-strain state of the track at a certain point in time, change of these parameters in time when a moving load passes this section and especially in the area of unevenness is also of no less interest. In this regard, the calculation program provides for obtaining of results showing record of parameters of the stress-strain state of the track under the point of load application. In addition, forces that arise at the point of contact of the wheel and the rail were obtained (Fig. 6). For ease of visualization, deflections of rails, ballast and ballast bed were placed with different initial ordinates.

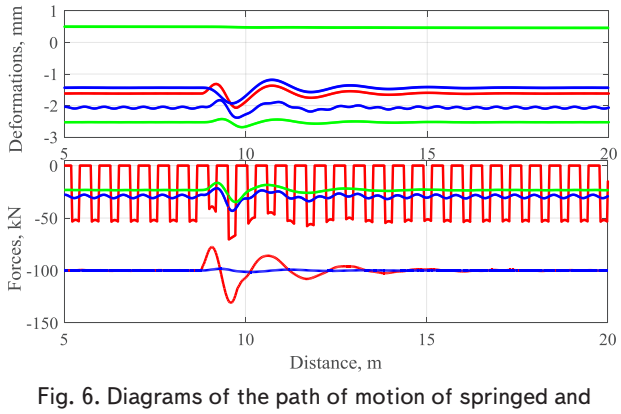

Fig. 6. Diagrams of the path of motion of springed and non-springed masses, deflections of the track elements under the point of contact of the wheel and the rail and corresponding loads

As can be seen from Fig. 6, dynamic deformations occurring in the ballast bed measured 0.3 mm and those in the ballast measured 0.8 mm. Forces in the point of contact between the wheel and the rail reached 137 kN. The obtained values of additional dynamic deflections and loads corresponded to those obtained according to the normative procedures of strength calculation of the track [7], that is, they were adequate for the set initial data.

On the basis of the developed model of short-term dynamic interaction of the track and the rolling stock, in addition to the rolling stock speeds, axial loads, over-spring and under-spring masses, it is also possible to take into consideration service performance indicators of the rolling stock. This is possible due to introduction of geometry of the wheel and the rail contact, equivalent conicity and modeling of transverse vibrations of the wheel pairs and the carriage.

5. Calculation of the residual subsidence of the ballast layer under the influence of multiple cyclic and short-term dynamic loads

Let us simulate the ballast effect on the track geometry impairment for various sleeper diagrams following the above methods. Simulation results are shown as a set of lines each showing subsidence of the track after passing a certain number of load axles. Subsidence of the track caused by impairment of the ballast layer for a standard sleeper diagram of 1,840 pcs/km is shown in Fig. 7 and those for 1,680 pcs/km and 1,440 pcs/km are shown Fig. 8, 9, respectively.

It is seen from Fig 7 that development of the ballast layer subsidence increases with the growth of the passed tonnage. There is a simultaneous overall subsidence of the track and accelerated development of subsidences near the unevenness. Development of unevenness occurs not only directly in the point of initial unevenness but also outside this zone. At the same time, unevenness extends both in the direction of the load movement and also in a reverse direction. Initial unevenness is gradually smoothed out and its maximum value is shifted relative to the initial direction of the load movement.

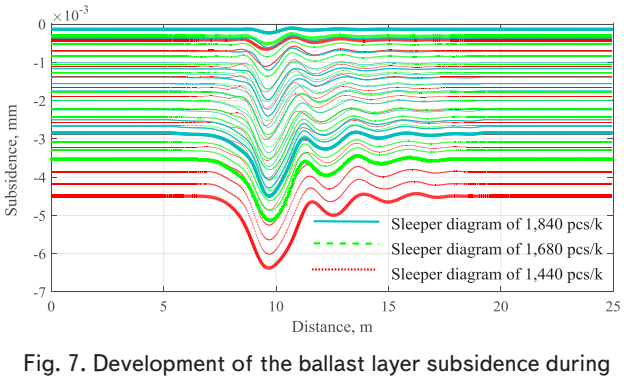

Fig. 7. Development of the ballast layer subsidence during passage of 2 million axles for sleeper diagrams of 1,840 pcs/ km, 1,680 pcs/km and 1,440 pcs/km

According to the developed model, if subsidence of the ballast layer is not compensated by elastic deflections of rails and sleepers, they cause an uneven change of elasticity along the track. Fig. 8 shows the diagram of elasticity distribution in the track for the sleeper diagram of 1840 pcs/km after passage of 2 million axles. When geometric unevenness is 9.27±0.5 m, the wave of significant decrease in elasticity is located predominantly to the right of initial unevenness and reaches 6 m. The decrease in elasticity caused by appearance of the gap results in less intensive accumulation of deformations in the zone of geometric unevenness and an increased growth at the sides of subsidence unevenness.

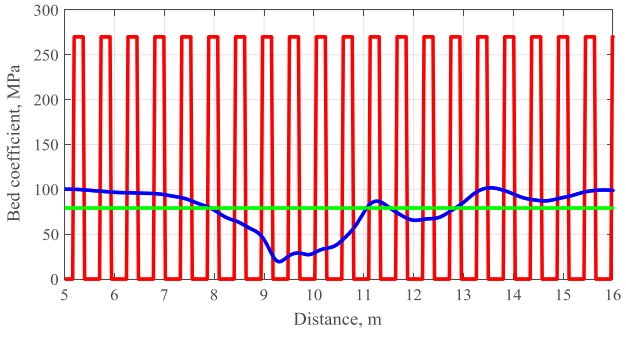

Fig. 8. Diagram of elasticity distribution in the track for the sleeper diagram of 1,840 pcs/km after passage of 2 million axles

Such nonuniformity of elasticity manifests itself in the form of uneven deflection of rails during rolling of a wheel which leads to occurrence of force unevenness under load. To estimate the impact of the ballast layer subsidence on the force unevenness of the track, deformations in the presence of only a static moving load are calculated. Fig. 9 shows elastic subsidence of the rail without geometric unevenness under a static moving load on a track for sleeper diagrams of 1,840 pcs/km, 1,680 pcs/km and 1,440 pcs/km after passage of 0, 5,000, 50,000, 500,000, 1,000,000 and 2,000,000 axles.

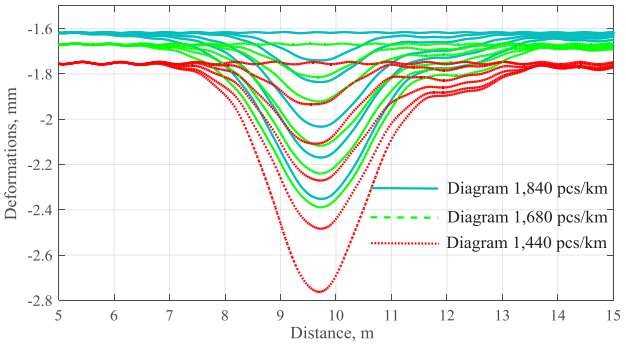

Fig. 9. Diagram of elastic subsidences under a static moving load on the track for sleeper diagrams of 1,840 pcs/km, 1,680 pcs/km and 1,440 pcs/km after passage of 0. 5,000, 50,000, 500,000, 1,000,000 and 2,000,000 axles

For estimation of the level of force interaction, the change in the stress-strain state of the track on the end of unevenness for sleeper diagrams of 1,840 pcs/km, 1,680 pcs/km and 1,440 pcs/km and on the nonlinearities that arose after passage of 2 million axles was shown. The comparison was made at maximum values that arose because of dynamic oscillations. The results of comparing the force action of the carriage on the track for various sleeper diagrams are given in Table 1.

Fig. 10 shows a change in the depth of unevenness during the entire tonnage passage for three sleeper diagram variants.

Despite the fairly small difference between unevennesses for different sleeper diagrams, large values of the passed tonnage correspond to this difference. Development of unevenness at the sleeper diagram of 1,440 pcs/km is much faster than at 1,680 pcs/km and 1,840 pcs/km. When unevenness at the sleeper diagram of 1,840 pcs/km reaches a certain depth after passage of 2 million axles, the same depth of unevenness in the track at the diagram of 1,680 pcs/km is achieved after passage of 1.38 million axles and following passage of 0.65 million axles at the sleeper diagram of 1,440 pcs/km. A similar conclusion was also drawn based on the results of calculations at a static load with the use of the law of the fourth degree [4, 13, 15] at which impairment accelerates by 34 % when pressure on the ballast increases by 11 % and in transition to the sleeper diagram of 1,680 pcs/km. In transition to the sleeper diagram of 1,440 pcs/km, time between waddings reduces to 32 % compared with the sleeper diagram of 1,840 pcs/km.

Table 1

Comparison of the carriage force action on the track for sleeper diagrams of 1,840 pcs/km, 1,680 pcs/km and 1,440 pcs/km on unevenness that arose after passage of 2 million axles

Indicators	Sleeper diagram of 1,840 pcs/km	Sleeper diagram of 1,680 pcs/km	%	Sleeper diagram of 1,440 pcs/km	%
Normal stresses in the rail σ, MPa	68.3	72.95	6	85.32	25
Force acting on the ballast P_b, kN	42.82	48.05	11	58.89	38
Force acting on the rail P, kN	120.4	130.1	8	139.7	16
Intensity of unevenness development, mm/1 mln. t	0.149	0.183	23	0.266	79

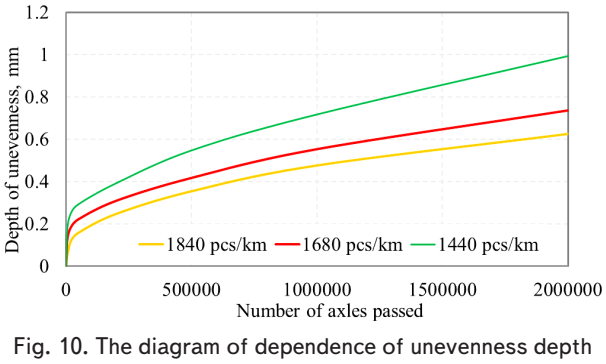

Fig. 10. The diagram of dependence of unevenness depth resulted from the ballast layer impairment on the number of axles and the amount of load for sleeper diagrams of 1,440 pcs/km, 1,840 pcs/km and 1,680 pcs/km

6. Discussion of results obtained in the study to form assessment of the track strength state

Residual deformations of the ballast layer cause appearance of a gap along edges of the sleepers which can grow into a complete loss of contact between the bottom surface of sleepers and the ballast. Various contact cases may take place depending on the loads acting on the track and deformation of rails and sleepers. The gap can be completely closed under the loads that are sufficiently large to cause sleepers displacement larger than the ballast subsidence. Incomplete closure of the gap or even absence of contact is possible at lower loads. Thus, the gaps under the sleepers

have a significant effect on redistribution of loads among the neighboring sleepers.

It was assumed that the track unevenness caused by the ballast layer subsidence at low velocities leads just to appearance of additional dynamic pressure on the ballast but does not have an effect on the vibration action. Also, internal factors have a mutual influence on each other. For example, the vibration load factor has an effect on intensity of subsidence accumulation only in presence of the factor of pressure on the ballast layer but not vice versa.

Despite the fairly small difference between unevennesses at different sleeper diagrams, rather large values of the passed tonnage may correspond to this difference. This is demonstrated by the diagram of growth of the unevenness depth depending on the passed tonnage for various sleeper diagrams. Development of unevenness at the sleeper diagram of 1,680 pcs/km is faster than that for the sleeper diagram of 1,840 pcs/km and much faster for the sleeper diagram of 1,440 pcs/km. When unevenness for the sleeper diagram of 1,840 pcs/km reaches a certain depth after passage of 2 million axles, the same depth for the sleeper diagram of 1,680 pcs/km is achieved after passage of 1.38 million axles and for the sleeper diagram of 1,440 pcs/km after 0.65 million axles passed. The accelerated development of unevenness in transition to the less dense sleeper diagram is explained by two causes. The first of them is a disproportionately rapid increase in intensity of accumulation of residual subsidence with an increase in pressure on the ballast layer. The second is rapid growth of dynamic loading of the track with growth of the track unevenness.

An important role is played by the initial geometric unevenness of the track which, despite relatively small dimensions, causes vibratory dynamic loads which, in turn, increase intensity of accumulation of residual deformations. The urgent task of further studies consists in establishing admissible limits of track maintenance and operating conditions for a structure with a less dense sleeper diagram at which intensity of impairment would still be at an acceptable level. For example, timely removal of geometric unevenness on rails by means of grinding and surfacing could prevent development of unevenness caused by subsidence of the ballast layer and significantly delay the term of the next track wadding. This is especially true for the sparse sleeper diagram of 1,440 pcs/km which is extremely sensitive to dynamic loads according to the results of this study.

From the point of view of practical use, the developed design diagram has limitations. These limitations consist in complexity of determining and specifying actual values of the ballast layer pollution and humidity and setting the magnitude of short unevennesses bringing about impact-vibrational action. The obtained results in aggregate are essential for the railroad transport industry.

7. Conclusions

1. A procedure for forecasting impairment of the track geometry was developed which, in contrast to the existing methods, takes into consideration variation of the stress-deformation state of the ballast layer depending on the track design, elasticity of the ballast bed, vibrational effect of the rolling stock, etc. This makes it possible to further expand the range of tasks of applying this procedure to the following pressing problems: optimal selection of parameters of the track design for given operating conditions, establishment of admissible speeds and loads of the rolling stock to provide acceptable inter-repair terms, etc. The existing procedures which do not differentiate influence of the track design, the ballast bed and characteristics of the rolling stock do not enable all-round solution of these problems.

2. The process of impairment of the track geometry in the zone of short geometric unevennesses is accompanied by uneven subsidence of the rail-sleeper grid with appearance of gaps under individual sleepers. This results in a change of elasticity along the track which causes slowdown in the growth of dynamic loads in the gap zone. At the same time, redistribution of loads among the sleepers neighboring with gap occurs. This approach can explain development of unevennesses not only directly in the zone of initial unevenness but also outside this zone. At the same time, unevenness extends both in the direction of the load movement and in the reverse direction. Initial unevenness is gradually smoothed out and its maximum value is shifted relative to the initial direction of the load movement.

3. According to the developed calculation procedure, impairment of the track geometry caused by subsidence of the ballast layer with a sparse sleeper diagram was calculated. When switching to the sleeper diagram of 1,440 pcs/km, static load from sleepers to the ballast increases by 21 % and the time between the ballast wadding decreases by 32 % as compared to the 1,840 pcs/km.

References

1. The complex phenomenological model for prediction of inhomogeneous deformations of railway ballast layer after tamping works / Sysyn M., Gerber U., Kovalchuk V., Nabochenko O. // Archives of Transport. 2018. Vol. 47, Issue 3. P. 91–107. doi: https://doi.org/10.5604/01.3001.0012.6512
2. Lichtberger B. Handbuch Gleis: Unterbau, Oberbau, Instandhaltung, Wirtschaftlichkeit. Hamburg: Tetzlaff Verlag, 2003. 562 p.
3. Lichtberger B. Track Compendium. Eurailpress Tetzlafl-Hestra GmbH & Co. KG, 2005. 634 p.
4. Gerber U. Setzungsverhalten des Schotters // Železniční dopravní cesta. Sborník přednášek. Decin, 2010. P. 117–122.
5. Gerber U., Fengler W. Setzungsverhalten des Schotters // Eisenbahntechnische Rundschau. 2010. Issue 4. P. 170–175.
6. Theoretical study into efficiency of the improved longitudinal profile of frogs at railroad switches / Kovalchuk V., Sysyn M., Sobolevska J., Nabochenko O., Parneta B., Pentsak A. // Eastern-European Journal of Enterprise Technologies. 2018. Vol. 4, Issue 1 (94). P. 27–36. doi: https://doi.org/10.15587/1729-4061.2018.139502
7. Danilenko E. I., Rybkin V. V. Pravyla rozrakhunkiv zaliznychnoi koliyi na mitsnist i stiykist (TsP/0117). Zatverdzheno nakazom Ukrzaliznytsi vid 13.12.2004 r. No. 960 TsZ. Kyiv: Transport Ukrainy, 2006. 168 p.

8. Esveld C. Modern railway track. MRT-Production, 2001. 653 p.
9. Particle filter-based prognostic approach for railway track geometry / Mishra M., Odelius J., Thaduri A., Nissen A., Rantatalo M. // Mechanical Systems and Signal Processing. 2017. Vol. 96. P. 226–238. doi: https://doi.org/10.1016/j.ymssp.2017.04.010
10. Fischer S. Breakage test of railway ballast materials with new laboratory method // Periodica Polytechnica Civil Engineering. 2017. Vol. 61, Issue 4. P. 794–802. doi: https://doi.org/10.3311/ppci.8549
11. Németh A., Fischer S. Investigation of glued insulated rail joints with special fiber-glass reinforced synthetic fishplates using in continuously welded tracks // Pollack Periodica. 2018. Vol. 13, Issue 2. P. 77–86. doi: https://doi.org/10.1556/606.2018.13.2.8
12. Sysyn M. P., Kovalchuk V. V., Jiang D. Performance study of the inertial monitoring method for railway turnouts // International Journal of Rail Transportation. 2018. P. 1–14. doi: https://doi.org/10.1080/23248378.2018.1514282
13. Nielsen J. C. O., Li X. Railway track geometry degradation due to differential settlement of ballast/subgrade – Numerical prediction by an iterative procedure // Journal of Sound and Vibration. 2018. Vol. 412. P. 441–456. doi: https://doi.org/10.1016/j.jsv.2017.10.005
14. Holtzendorff K. Untersuchung des Setzungsverhaltens von Bahnschotter und der Hohllagenentwicklung auf Schotterfahrbahnen. Dissertation. Technische Universität Berlin. Berlin, 2003. 130 p.
15. Lysyuk V. S., Sazonov V. N., Bashkatova L. V. Prochnyy i nadezhnyy zheleznodorozhnyy put'. Moscow: IKC «Akademkniga», 2003. 589 p.
16. Die Instandhaltung der Bettung / Nabochenko O., Sysyn M., Gerber U., Rybkin V. // Železniční Dopravní Cesta. Děčín, 2011. P. 23–32.
17. Dynamical response of railway switches and crossings / Salajka V., Smolka M., Kala J., Plášek O. // MATEC Web of Conferences. 2017. Vol. 107. P. 00018. doi: https://doi.org/10.1051/matecconf/201710700018
18. Estimation of carrying capacity of metallic corrugated structures of the type Multiplate MP 150 during interaction with backfill soil / Kovalchuk V., Kovalchuk Y., Sysyn M., Stankevych V., Petrenko O. // Eastern-European Journal of Enterprise Technologies. 2018. Vol. 1, Issue 1 (91). P. 18–26. doi: https://doi.org/10.15587/1729-4061.2018.123002
19. Kassa E. Dynamic train-turnout interaction: mathematical modelling, numerical simulation and field testing. Chalmers University of Technology, Göteborg, 2007.
20. Myamlin S. V. Modelirovanie dinamiki rel'sovyh ekipazhey. Dnepropetrovsk: Novaya ideologiya, 2002. 240 p.
21. Met'yuz D. G., Fink K. D. Chislennye metody. Ispol'zovanie MATLAB. Moscow: Izdatel'skiy dom «Vil'yams», 2001. 720 p.